

THE INFLUENCE OF GEOTECHNICAL VARIABILITY IN THE SUBSIDENCE CAUSED BY URBAN TUNNEL EXCAVATION

Miranda, Luís, *LNEC, Lisboa, Portugal, lmiranda@lnec.pt*

Bilé Serra, João, *LNEC, Lisboa, Portugal, biles@lnec.pt*

Caldeira, Laura, *LNEC, Lisboa, Portugal, laurac@lnec.pt*

ABSTRACT

Initially, the subsidence geometry due to tunnelling is described using an empirical Gaussian function. Then, an analytical expression for estimating the displacement field is discussed, considering the effects of ovalization and pure contraction of the tunnel. The Random Field Theory is briefly introduced in order to characterize statistically the geotechnical parameters, taking into account the ground variability and its spatial correlation properties. Subsequently, two software tools are developed to analyze the settlements caused by tunnelling. The first one is based on the Monte Carlo method and is applied to statistical analysis of subsidence basins. The second one is based on the generation of spatially correlated random fields and allows assessing the influence of the ground spatial variability on the dispersion of surface settlements. Finally, the numerical results are compared with observational results from a real tunnel.

1. INTRODUCTION

Ground settlements caused by the excavation of tunnels may be particularly relevant in urban areas, with greater significance in soft soils. Estimating the amplitude of the settlements and the associated risk to buildings is an essential part of tunnel planning, design and construction. Empirical and analytical models are currently used. However, the ground local variability and its spatial variability are not generally considered. Among other factors, the quality of the settlement estimates depends on the amplitude of both types of variability. The quantification of ground variability improves the robustness of the forecasts. This is of paramount importance to the definition of warning and alarm limits for risk management during tunnel construction.

2. SURFACE SETTLEMENTS DUE TO TUNNEL EXCAVATION

The geometry of the subsidence basin and the amplitude of surface settlements caused by underground excavation can be estimated with a reasonable degree of confidence for the green field situation. Empirical correlations based on field observations are currently used for this estimation. In Figure 1 the geometry of the subsidence basin is outlined, with a reference system xyz , in which x and z are the horizontal and vertical axes in the plane of the face and y is the longitudinal axis. The vertical displacement is designated by S_v and the horizontal displacements, in the transverse and longitudinal direction, by S_{hx} and S_{hy} .

Schmidt (1969) and Peck (1969) suggested, after analysing a considerable number of case records, that the cross-sectional area of subsidence at the surface is well described by a Gaussian function:

$$S_v(x) = S_{v,\text{máx}} e^{-\frac{x^2}{2i_x^2}} \quad [1]$$

where $S_{v,\text{máx}}$ is the peak settlement over the tunnel axis. The parameter i_x stands for the distance between the plane of symmetry of the tunnel and the inflexion points of the theoretical subsidence curve.

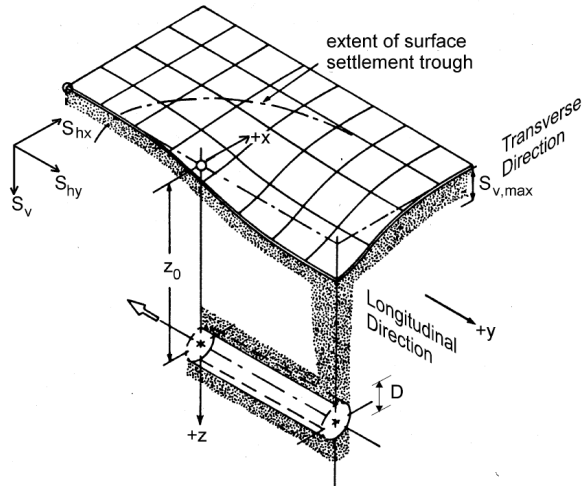


Figure 1 – Geometry of the subsidence basin (Franzius, 2003)

The use of elastoplastic models, either analytical or numerical, for modelling the subsidence pattern is strictly required by the non-linearity and partial irreversibility of deformation that characterizes the mechanical response of the ground. At sufficiently distant positions from the excavation, however, the use of elastic models based on an estimate of the ground loss may be appropriate. Several models may be found in the literature such as the one by Sagaseta (1987), for ground loss estimate due to tunnel construction (valid for a constant volume condition), which was later extended by Verruijt and Booker (1996) to allow the use of an arbitrary value of the Poisson's ratio. In this extended solution the joint effects of radial contraction and ovalization of the tunnel are considered.

Loganathan and Poulos (1998) further developed the solution by Verruijt and Booker and defined an equivalent parameter ϵ_{eq} , which is related to the pure contraction of the tunnel as well as to the nonlinear ground movement due to the tunnel ovalization. It is based on the gap parameter g introduced by Rowe and Knack (1983) which, according to Lee *et al.* (1992), results from the combined effects of three-dimensional elastoplastic deformations at the tunnel face, from the soil over-excavation and also from the gap due to the conical shape of the tunnelling machine. The undrained surface settlement is then equal to

$$S_v(z=0) = 4(1-\nu)R^2 \frac{z_0}{x^2 + z_0^2} \frac{4gR + g^2}{4R^2} \exp\left[-\frac{1.38x^2}{(z_0 + R)^2}\right] \quad [2]$$

3. ASSESSMENT OF THE GROUND GEOTECHNICAL PROPERTIES VARIABILITY

The variability of the soil is caused by natural geological processes. It can be observed locally – statistical variability – or by considering the values in several positions – spatial variability. The spatial variability of the ground can be modelled taking into account two contributions: an identified deterministic trend and a residual variability about that trend, which characterizes the inherent variability of the soil deposit. For the one-dimensional model case, the local value of the property $z(x)$ can be represented by:

$$z(x) = t(x) + u(x) \quad [3]$$

in which $t(x)$ is the value of the statistical trend at x and $u(x)$ is the residual variation, supplementary to the tendency. The residuals are characterized statistically as a random variable, with zero mean, and variance:

$$\text{Var}(u) = E\left[\{z(x) - t(x)\}^2\right] \quad [4]$$

The remaining spatial structure, after removing the trend, shows the existence of correlation among the residuals, i.e., the residuals aren't statistically independent. This spatial structure of variation, unconsidered by the trend, may be described by the spatial correlation, usually called autocorrelation, which depends on the distance between positions. The spatial association of residuals may be summarized by the autocorrelation function $R_z(\delta)$, which describes the correlation of $u(x_i)$ and $u(x_j)$ as separation distance δ increases:

$$R_z(\delta) = \frac{1}{\text{Var}[u(x)]} E[u(x_i)u(x_{i+\delta})] = \frac{C_z(\delta)}{\text{Var}[u(x)]} \quad [5]$$

in which $\text{Var}[u(x)]$ is the variance of the residuals and $C_z(\delta)$ is the autocovariance function of the residuals, at two positions separated by a distance δ . Therefore, the spatial variability about a trend is due to the variance (local effect) and to the autocorrelation (spatial effect).

In order to consider the ground spatial variability in models of surface settlements caused by tunnel excavation, it is necessary to resort to the Random Field Theory, considering that the generic variable $z(x)$ (e.g., the deformation modulus) is a realization of a stochastic scalar field. Its parameters are, thus, the mean μ_z , assumed constant, the variance σ_z^2 and the autocovariance function $C_z(\delta)$ (Baecher and Christian, 2003).

The average process in a reference length X is an essential resource in geotechnical modelling, allowing the definition of "homogeneous" sub-domains. As a matter of fact, the vast majority of the available information on geotechnical parameters in any site is defined over a finite domain and represents a local average of the parameter, instead of its exact local value. The spatial average of the process within the interval $[0, X]$ is:

$$M_X(z(x)) = \frac{1}{X} \int_0^X z(x) dx \quad [6]$$

The spatial averaging process smoothes the studied variables. Actually, the variance of the averaged process is smaller and its spatial correlation is wider than the original process $z(x)$. The corresponding 1st and 2nd order moments of the spatial mean can be determined from the mean and variance of the scalar process $z(x)$:

$$E[M_X] = \mu_{M_X} = \frac{1}{X} \int_0^X \mu_z dx = \mu_z \quad [7]$$

$$\text{Var}[M_X] = \frac{1}{X^2} \int_0^X \int_0^X C_z(x_i - x_j) dx_i dx_j = \frac{2}{X^2} \int_0^X (X - \delta) C_z(\delta) d\delta \quad [8]$$

The scale of fluctuation or (effective) correlation distance θ_z of the process $z(x)$ represents the distance above which the values of $R_z(\delta)$ are smaller than $1/e^2$, i.e. where no significant correlation exists. According to Vanmarcke (1984) the scale of fluctuation can be estimated by:

$$\theta_z = 2 \int_0^\infty R_z(\delta) d\delta = \int_{-\infty}^\infty R_z(\delta) d\delta \quad [9]$$

The variability of the ground, modelled using the Random Field Theory, can be described with the coefficient of variation ($\text{COV}_z = \sigma_z / \mu_z$) and the fluctuation scale θ_z . Although the spatial variability pattern of a given area is related with the specific regional geology, published values of the COV variation interval for geotechnical variables may be useful as an introductory guidance (see Table 1). Based on a limited data set, Phoon and Kulhway (1999) concluded that the ratio of the horizontal scale of fluctuation to the vertical one is close to 10, thus confirming

the greater importance of the latter. These authors suggest that typical values for the horizontal scale vary between 40 m and 60 m.

Numerical modelling of the spatial variability of geotechnical properties includes analyzing an adequate number of realizations, allowing one to assess the magnitude and statistical distribution of the corresponding effects. In order to generate the realizations $z(x)$, the fast Fourier transform method was selected, mainly because it is computationally efficient and, being a numerical technique, it can be used with any given covariance model.

Table 1 – Values of the estimates of statistical measures for some relevant parameters

Parameter	Reference	Variation interval	Mean value	COV variation interval (%)	COV mean value (%)
ϕ_{clay}	Lee <i>et al.</i> (1983)	-	-	[12,56]	-
	Phoon e Kulhawy (1999)	[9°,33°]	15.3°	[10,50]	21
	Phoon e Kulhawy (1999)	[17°,41°]	33.3°	[4,12]	9
$S_{u,\text{clay}}$	Lee <i>et al.</i> (1983)	-	-	[20,50]	30
	Phoon e Kulhawy (1999)*	[15,363] kPa	276 kPa	[11,49]	22
	Phoon e Kulhawy (1999)**	[130,713] kPa	405 kPa	[18,42]	32
ρ	Lee <i>et al.</i> (1983)	-	-	[1,10]	3
γ	Phoon e Kulhawy (1999)	[14,20] kN/m ³	17.5 kN/m ³	[3,20]	9
γ_d	Phoon e Kulhawy (1999)	[13,18] kN/m ³	15.7 kN/m ³	[2,13]	7
E	Lee <i>et al.</i> (1983)	-	-	[2,42]	30
E_{PMT}	Phoon e Kulhawy (1999)	[5.2,15.6] MPa	8.97 MPa	[28,68]	42

* Unconsolidated undrained triaxial test; ** Consolidated undrained triaxial test.

4. STATISTICAL VARIABILITY OF SETTLEMENTS

In order to analyze the displacements caused by tunneling, two case studies are herein described. In the first one, which corresponds to the TBM excavation of a circular tunnel in a moderately consolidated stiff clay ground, only the influence of the ground statistical variability is considered. That is to say, a homogeneous field with uniform properties throughout the model is created. Mathcad is used with the main purpose of randomly generating a set of deformation modulus corresponding to the number of simulations desired, according to a specific statistical distribution (Miranda, 2011). Then, using the analytical expression for obtaining the surface settlement of Loganathan and Poulos (1998), histograms and cumulative frequency curves of maximum settlement and subsidence volume are drawn.

The tunnel has a diameter of 10 m and is fully excavated above the water level, on the saturated fringe of the ground. Thus, an undrained behaviour is considered. The main purpose of this section is to evaluate the importance of the statistical variability of the ground undrained stiffness, E_u , in the surface settlements and in the shape of the subsidence curve. Nine calculation cases are then considered as shown in Table 2. 500 realizations of random numbers are generated according to a lognormal distribution, whose parameters are determined from the average value, μ_{E_u} , and its coefficient of variation, COV_{E_u} . The lognormal distribution is considered an appropriate distribution for modeling the variation of E_u , since it can only have positive values.

Figure 2 presents two graphs with examples of subsidence curves obtained for different realizations of E_u . As expected, the subsidence curve has a lower maximum settlement and is wider in the 2A case, in which the tunnel is deeper. In the latter case, the value of parameter i is 16.0 m while in the first case it is 11.1 m.

Table 2 – Calculation cases

Calculation case	Depth of the tunnel axis z_0	Undrained shear strength S_u	Average stiffness index $I_{r,m}$	Deformation modulus E_u	
				μ_{E_u}	COV_{E_u} (%)
1A1	20 m	100 kPa	125	37.5 MPa	20
1A2					10
1A3					30
1B1		50 kPa	150	22.5 MPa	20
1B2					10
1B3					30
2A	30 m	125 kPa	125	46.9 MPa	20
2B					10
2C					30

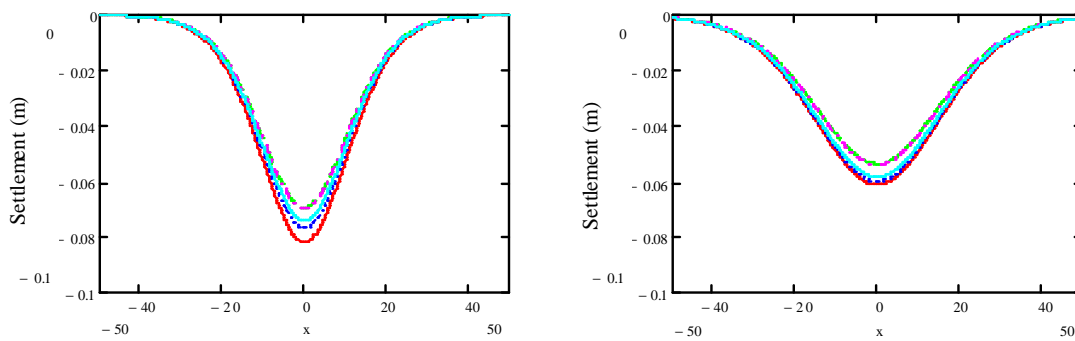


Figure 2 – Subsidence curves for calculation case 1A1 and 2A

Figure 3 shows the cumulative frequency curves for the various cases of calculation. The dashed curves, corresponding to cases 1A2, 1B2 and 2B, have a greater slope, indicating a smaller dispersion, given the lower value of the COV. The average settlement is higher for the cases in which the tunnel is closer to the surface (1A and 1B). The largest average settlement is associated with case 1B, given the lower deformation modulus of the ground.

The importance of the statistical variability of the ground increases with decreasing tunnel depth, to which also contributes the fact that the deeper tunnel induces lower settlements at the surface. Actually, comparing case 1A and case 2, whose ground parameters are similar, the dispersion is more evident in case 1A, in which the tunnel is closer to the surface. In Table 3 it can be seen, as well, that the highest values of COV correspond to a greater dispersion of the settlement values, increasing values of the 95% fractile and decreasing values of the 5% fractile of settlement. Table 3 also shows the lower and upper 5% fractiles of the subsidence volume.

Table 3 - Lower and upper 5% fractiles of the maximum settlement and subsidence volume

Lower fractile of 5%			Upper fractile of 5%		
Calculation case	Maximum settlement (m)	Subsidence Volume (m ³)	Calculation case	Maximum settlement (m)	Subsidence Volume (m ³)
1A1	0.064	1.798	1A1	0.079	2.206
1A2	0.068	1.892	1A2	0.075	2.087
1A3	0.062	1.736	1A3	0.085	2.372
1B1	0.087	2.422	1B1	0.093	2.604
1B2	0.088	2.463	1B2	0.091	2.541
1B3	0.086	2.393	1B3	0.095	2.663
2A	0.049	1.965	2A	0.060	2.400
2B	0.052	2.070	2B	0.058	2.347
2C	0.047	1.886	2C	0.061	2.463

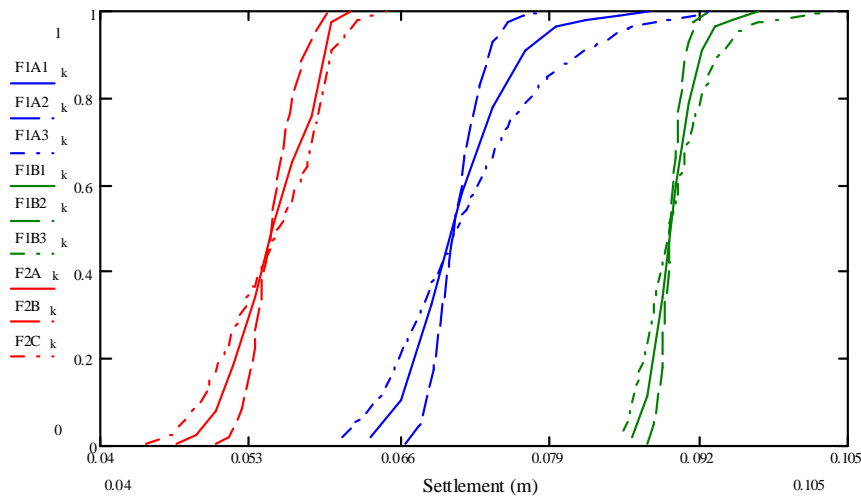


Figure 3 - Cumulative frequency curves for the various cases of calculation (maximum settlement)

Comparing Figure 3 with Figure 4, it is interesting to note that, in spite of the fact that the average settlement of case 2 is less than the one for case 1A, the volume of subsidence of case 2 is higher than the one for case 1A. This might be explained by the greater width of the subsidence surface in case 2, given the greater depth of the tunnel.

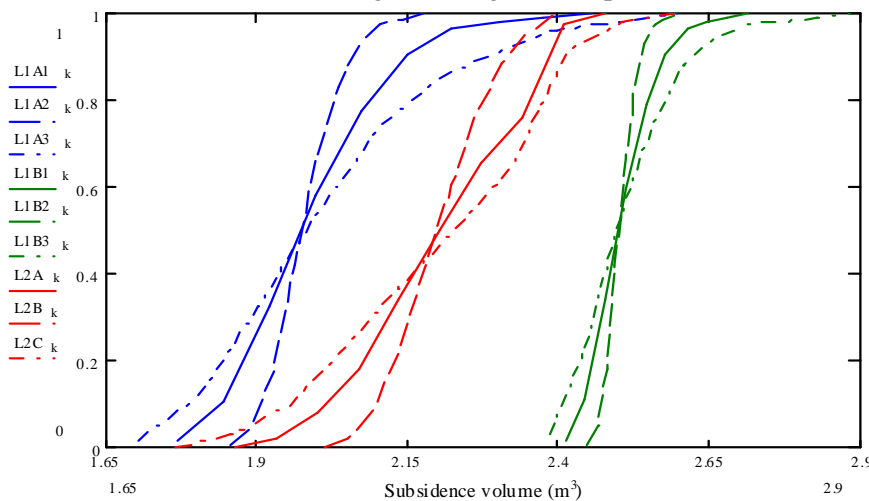


Figure 4 – Cumulative frequency curves for the various cases of calculation (subsidence volume)

5. SPATIAL VARIABILITY OF SETTLEMENTS

The second case considered is the excavation of the Alforneiros tunnel, which integrates the Lisbon subway blue line between Pontinha and Alforneiros, using the conventional method (NATM). In this case, a numerical example was created to analyze the influence of the ground spatial variability on the deformation around the tunnel opening and on the surface settlements. These variables play a key role in risk management during tunnel construction since alarm and alert behaviour limits are usually expressed in terms of settlement and convergence values.

An original MATLAB application was developed (Miranda, 2011). Basically, it consists of generating a matrix of realizations of a random scalar 2D field, using the fast Fourier transform method. A Gaussian model of local variability with negative exponential spatial correlation was adopted. Each column of the matrix (which corresponds to a realization of the random field) is stored in a file that is then read by FLAC 6.0. This program builds the fields $\phi(x)$ for the friction

angle and $E(x)$ for the deformation modulus, by translation of the mean and scaling of the standard deviation, assigning them to the elements of the mesh. After that, it generates the initial equilibrium, excavates the tunnel and places the support and gets the different results, which are written in the output files. Finally, the MATLAB application processes the results graphically, obtaining, for instance, statistical curves of settlements.

A numerical model of the tunnel, entirely excavated in the Benfica geological unit (Melâneo *et al.*, 2004), with an overburden of about 18.5 m, was considered in FLAC 6.0. The geometry of the model is presented in Figure 5. The tunnel cross-section has the geometry shown in Figure 6, with a maximum excavation radius of 4.95 m. The width of the model is 130 m to prevent the boundary conditions' effect on the tunnel response. Moreover, the distance of the tunnel center to the bottom boundary is three times the diameter.

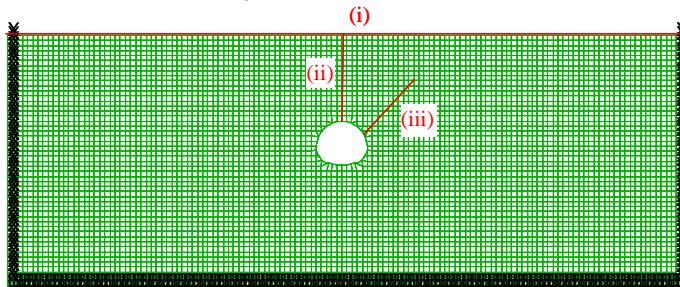


Figure 5– Geometric model

The ground corresponds to a stiff overconsolidated marl layer with a thickness of 50 m. A Mohr-Coulomb model was selected to simulate the behaviour of the ground, with cohesion of 50 kPa. Concerning the deformation modulus, the values considered for μ_E and COV_E were 150 MPa and 20%. In what regards the friction angle, the values assigned to μ_ϕ and COV_ϕ were 30° and 15%. The vertical scale of fluctuation adopted is 4 m and the horizontal is 40 m.

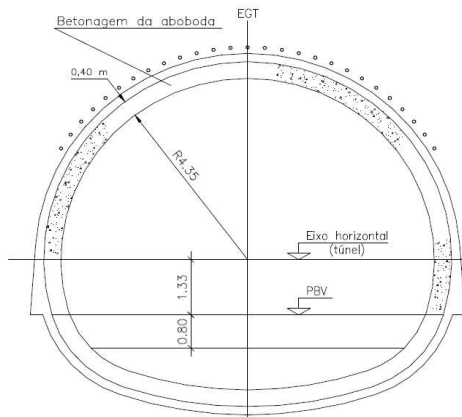


Figure 6 – Tunnel section (Melâneo *et al.*, 2004)

A total of five hundred realizations were generated, using MATLAB. In Figure 7, the values of the deformation modulus as well as of the friction angle are represented throughout the mesh for realization #53. It is assumed that there is total correlation between the two properties, which implies that the field $z(x)$, from which $\phi(x)$ and $E(x)$ are generated, is the same.

In what concerns the construction phases of the tunnel, the excavation was conducted in partial section (upper and lower half-section), under pre-support. The primary support adopted was shotcrete reinforced with welded-wire mesh with a thickness of 0.20 m and an elasticity modulus of 5 GPa and TH29 steel ribs, spaced 1.50 m. The advances on the upper half-section were 1.50 m, while those on the lower half-section were 4.50 m. Therefore, the following phases are defined in the numerical model: (i) initial equilibrium, (ii) excavation of the upper

section and partial relaxation of the top tunnel periphery, (iii) support installation in the upper section and relaxation until equilibrium is attained, (iv) excavation of the bottom section and partial relaxation of the lower tunnel boundary, (v) support installation in the lower section and relaxation until equilibrium is attained. In order to simulate relaxation, tensions were applied at the tunnel boundary to provide equilibrium at zero relaxation. In step (ii), a relaxation coefficient of 60% was considered suitable for modeling the behaviour of the ground before installing the support, taking into account the existence of pre-support, which contributes to a smaller displacement of the ground. In step (iv), a relaxation coefficient of 50% was applied for the lower half-section, which is lower than the one for the upper half-section, given the time lag between the excavation of the former and the latter.

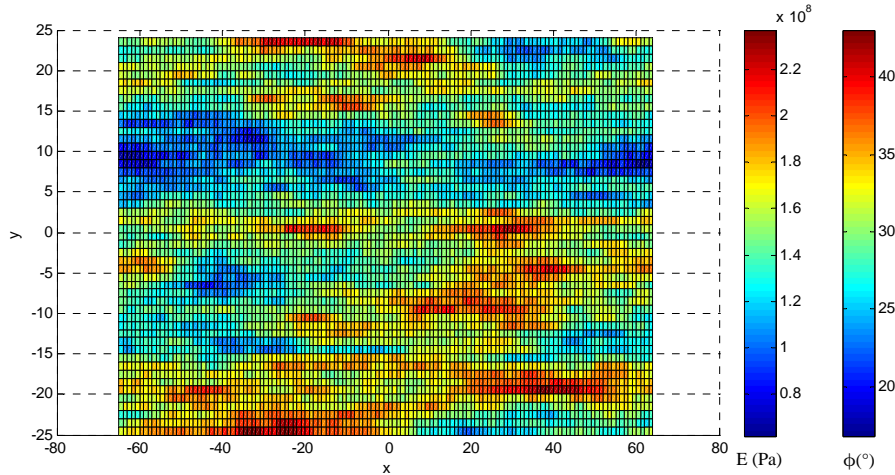


Figure 7 – Deformation modulus and friction angle (respectively) for realization #53: $\theta_z = 4$ m

Melâneo *et al.* (2004) obtained values for the surface settlements and evaluated the ground loss, based on an observation program that involved the installation of surface marks, inclinometers and strain gauges. These values allowed them to define the associated subsidence curve, which is represented in Figure 8 for the studied section of the tunnel (4A) (adjusted Gauss curve).

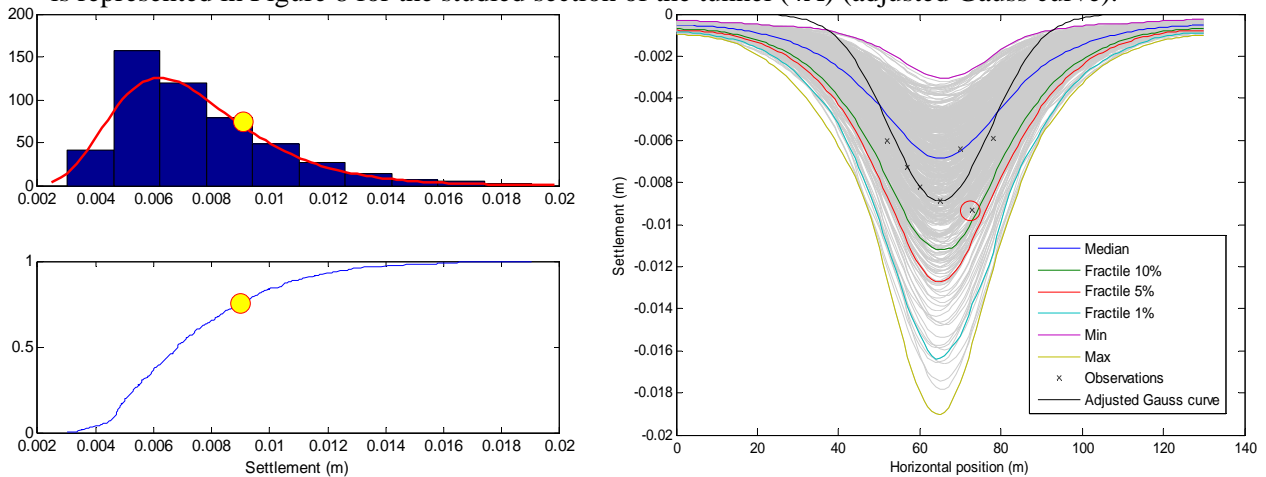


Figure 8 – Histogram and cumulative frequency curve of the maximum surface settlement (left) and statistical curves for the surface settlement (right)

The upper 5% fractile of maximum vertical surface settlement, maximum vertical displacement (at the tunnel crown) and maximum 45° displacement (at the tunnel wall) corresponds to a value of 1.3 cm, 2.2 cm and 2.1 cm, respectively. In Figure 8 to Figure 10, the histogram, cumulative frequency curve and lognormal adjusted distribution of the maximum surface settlement, the maximum vertical displacement and the maximum 45° displacement are presented, as well as

the associated statistical curves along (i), (ii) and (iii) (according to Figure 5), allowing a better understanding of these values. A significant scatter was obtained for the settlement curve at the surface, the settlement profile from the tunnel crown to the surface and the oblique radial displacement profile. This scatter shall be considered when defining the alarm and alert limits for the tunnel excavation. As a matter of fact, the peak surface settlement varies between 3 and 19 mm, the crown settlement between 8 and 31 mm and the radial displacement between 8 and 29 mm.

Comparing the numerical results with the observational results, the maximum observed surface settlements are below the upper 10% fractile of the numerical results. It is therefore concluded that the use of numerical models, that take into account the spatial variability of the ground, explains the results from observation. This is particularly true in the case of surface settlements, since the observed values are limited by the statistical curves of the median and of the upper 10% fractile in Figure 8. The fact that the observed values are above the median is mainly explained by the larger width of the numerical model curves (when compared to the real ones), leading to a lower value of the maximum settlement. Either way, the possibility of finding ground with worse characteristics in terms of strength and deformability (except for any ground singularity), is envisaged by the consideration of spatial variability.

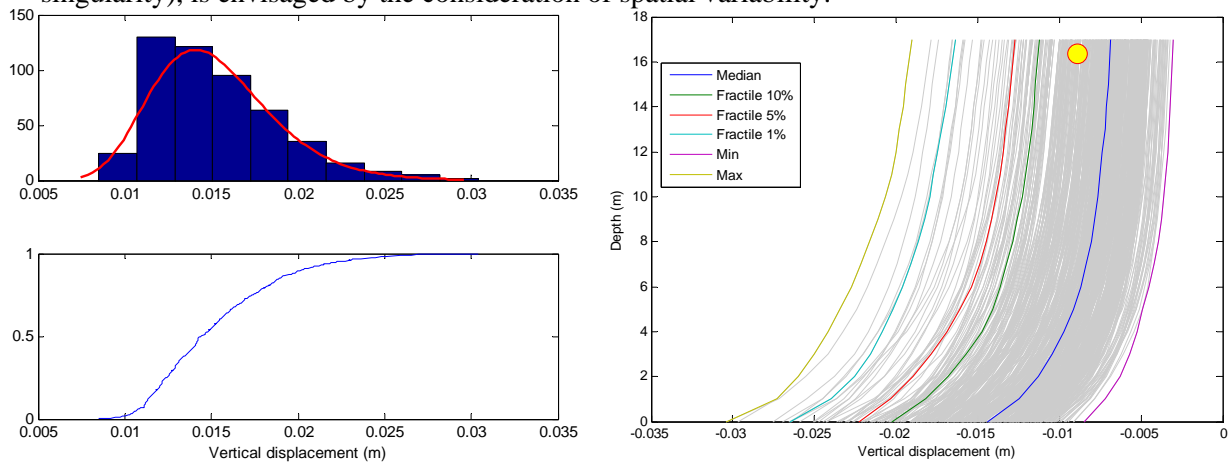


Figure 9 – Histogram and cumulative frequency curve of the maximum vertical displacement (left) and statistical curves for the vertical displacement (right)

6. FINAL CONSIDERATIONS

The present article addressed the issue of surface settlement caused by tunnelling, given the local and spatial statistical variability of the ground geotechnical parameters. In what concerns the local variability, statistical analysis of the subsidence curves, in terms of settlement and maximum amount of subsidence, suggests that the statistical variability of the ground is more important for shallow tunnels. Regarding the spatial variability, the adopted methodology allows the establishment of characteristic values – upper fractiles – which are useful in defining the criteria for risk management during tunnel construction, when no rupture of the excavation occurs. The case study shows that this methodology is appropriate in predicting the settlements, since it can explain the dispersion in the observed results.

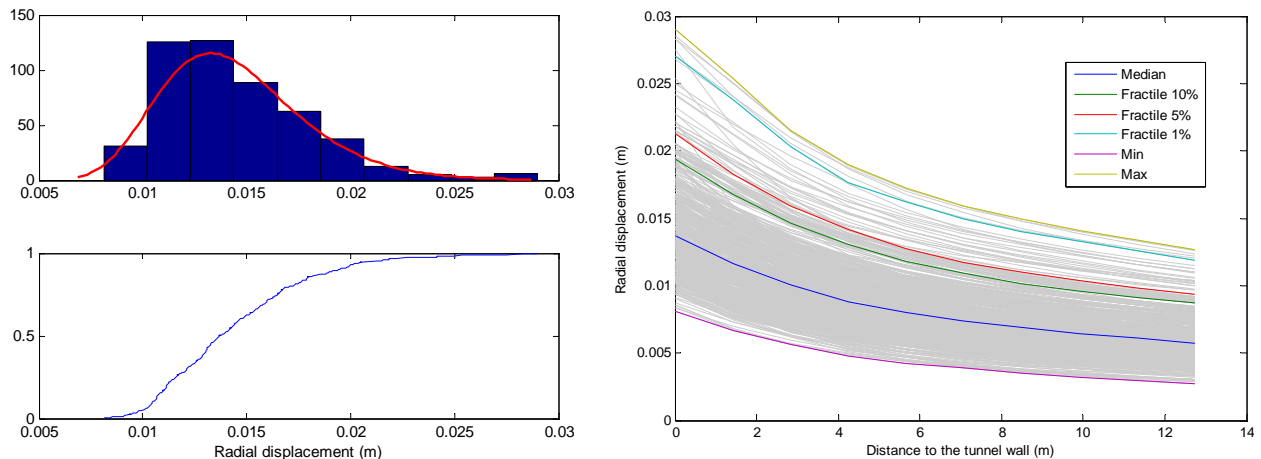


Figure 10 – Histogram and cumulative frequency curve of the maximum 45° displacement (left) and statistical curves for the 45° displacement (right)

REFERENCES

- Baecher, G. B., Christian, J. T. (2003). *Reliability and statistics in geotechnical engineering*. John Wiley & Sons, Inc., New Jersey, USA.
- Franzius (2003). *Behaviour of buildings due to tunnel induced subsidence*. Ph. D. Thesis, Department of Civil and Environmental Engineering, Imperial College of Science, Technology and Medicine, London.
- Lee, I. K., White, W. and Ingles, O. G. (1983). *Geotechnical Engineering*. Pitman, Boston.
- Lee, K. M., Rowe, R. K., Lo, K. Y. (1992). *Subsidence owing to tunnelling. I: Estimating the gap parameter*. Canadian Geotechnical Journal, Ottawa, Canada, 29, 929-940.
- Loganathan, N., Poulos, H. G. (1998). *Analytical prediction for tunneling-induced ground movements in clays*. Journal of Geotechnical and Geoenvironmental Engineering, 124(9). 846-856.
- Lumb, P. (1974). *Application of statistics in soil mechanics*. Soil Mechanics: New Horizons. Lee, I. K., ed., London, Newnes-Butterworth, 44-112, 221-239.
- Melâneo, F., Jorge, C., Diniz Vieira, G. (2004). *Escavação de túneis do Metropolitano de Lisboa na Formação de Benfica. Análise dos assentamentos e aferição de parâmetros*. IX Congresso Nacional de Geotecnia, 3, 553-564.
- Miranda, L. (2011). *Influência da variabilidade geotécnica na subsidência devida à escavação de túneis urbanos*. Dissertação para obtenção do grau de Mestre em Engenharia Civil. Instituto Superior Técnico.
- Peck, R. B. (1969). *Deep excavations and tunneling in soft ground*. Proceedings of the 7th int. Conference on Soil Mechanics and Foundation Engineering. State of the art volume. 225-290. Sociedad Mexicana de Mecanica de Suelos, A. C.
- Phoon, K-K., Kulhawy, F. H (1999). *Characterization of geotechnical variability*. Canadian Geotechnical Journal, 36, 612-624.
- Rowe, R. K., Knack, G. J. (1983). *A theoretical examination of the settlements induced by tunnelling: Four case histories*. Can. Geotech. J., Ottawa, Canada, 20, 299-314.
- Sagaseta, C. (1987). *Analysis of undrained soil deformation due to ground loss*. Géotechnique 37(3), 301-320.
- Schmidt, B. (1969). *Settlements and ground movements associated with tunnelling in soil*. Ph. D. Thesis, University of Illinois.
- Vanmarcke, E. (1984). *Random Fields: Analysis and Synthesis*, MIT Press, Cambridge, MA.
- Verruijt, A., Booker, J. R. (1996). *Surface settlements due to deformation of a tunnel in an elastic half plane*. Géotechnique 46(4), 753-756.